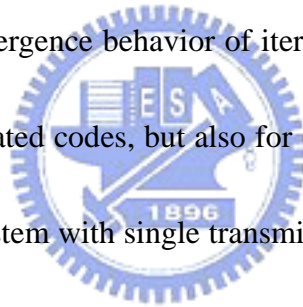


Chapter 4

Extrinsic Information Transfer (EXIT) Charts

In this chapter, we discuss one tool to analyze the convergence behavior of iterative processing. S. ten Brink [7] proposed the extrinsic information transfer (EXIT) charts in 2001. In [7], the author used the mutual information of output extrinsic log-likelihood ratios of the decoders of the parallel concatenated code. Using mutual information transfer characteristics of soft-in/soft-out decoders can help us better understanding the convergence behavior of iterative decoding schemes. This is not only for parallel concatenated codes, but also for serial concatenated codes. Here, we use serial concatenated system with single transmit and receive antenna in AWGN channels as example.



4.1 Transfer characteristics

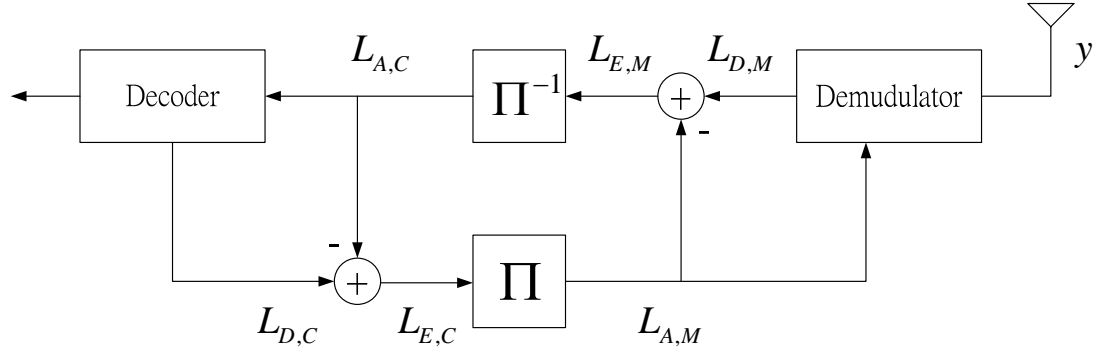


Fig. 4-1: Receiver diagram of a serial concatenated system

The serial concatenated system we consider is shown in Fig.4-1. To simplify the problem, we use BPSK in a single-input/single-output system. The received signal y from AWGN channel is

$$y = x + n \quad (4.1)$$

where n is the AWGN noise with zero mean and variance σ_n^2 , x is transmitted signal with BPSK. Then the conditional probability is

$$p(y | X = x) = \frac{1}{\sqrt{2\pi}\sigma_n} \exp\left(-\frac{(y-x)^2}{2\sigma_n^2}\right) \quad (4.2)$$

The corresponding log-likelihood ratios (LLRs) are

$$\begin{aligned} L_y &= \log \frac{p(y | x = +1)}{p(y | x = -1)} \\ &= \frac{2}{\sigma_n^2} \cdot y = \frac{2}{\sigma_n^2} \cdot (x + n) = \mu_y \cdot x + n_y \end{aligned} \quad (4.3)$$

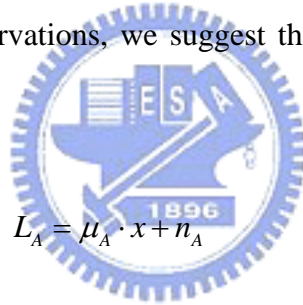
where $\mu_y = 2/\sigma_n^2$, and n_y is Gaussian distributed with zero mean and variance

$$\sigma_y^2 = 4 / \sigma_n^2 \quad (4.4)$$

Two observations in [7]:

1. If interleavers is large, the a priori LLR remain fairly uncorrelated from the respective channel observations L_y over many iterations.
2. The PDFs of the extrinsic outputs approach Gaussian-like distribution with increasing number of iterations .

From the above two observations, we suggest that the a priori LLR L_A can be modeled as (4.3)



$$L_A = \mu_A \cdot x + n_A \quad (4.5)$$

and

$$\mu_A = \sigma_A^2 / 2 \quad (4.6)$$

So the PDF of L_A is

$$p_A(\xi | X = x) = \frac{1}{\sqrt{2\pi}} \exp \left[-\frac{\left(\xi - \frac{\sigma_A^2}{2} \cdot x \right)^2}{2\sigma_A^2} \right] \quad (4.7)$$

Mutual information $I_A = I(X; L_A)$ [17] between transmitted bits X and a priori LLR L_A is

$$I_A = \frac{1}{2} \sum_{x=-1,1} \int_{-\infty}^{\infty} p_A(\xi | X = x) \cdot \log_2 \left(\frac{2 \cdot p_A(\xi | X = x)}{p_A(\xi | X = 1) + p_A(\xi | X = -1)} \right) \quad (4.8)$$

$$0 \leq I_A \leq 1$$

with the consistency condition [18] for the LLR

$$p_A(\xi | X = x) = p_A(-\xi | X = x) \cdot e^{x\xi} \quad (4.9)$$

$$I_A(\sigma_A) = 1 - \int_{-\infty}^{\infty} \frac{\exp\left[-\frac{(\xi - \sigma_A^2/2)^2}{2\sigma_A^2}\right]}{\sqrt{2\pi}\sigma_A} \cdot \log_2(1 + e^{-\xi}) d\xi \quad (4.10)$$

because it is monotonically increasing in σ_A [17], σ_A can be obtained by

$$\sigma_A = J^{-1}(I_A) \quad (4.11)$$

then we have to calculate the mutual information of the output extrinsic LLR

$$I_E = I(X; L_E) = \frac{1}{2} \sum_{x=-1,1} \int_{-\infty}^{\infty} p_E(\xi | X = x) \cdot \log_2 \left(\frac{2 \cdot p_E(\xi | X = x)}{p_E(\xi | X = 1) + p_E(\xi | X = -1)} \right) \quad (4.12)$$

$$0 \leq I_E \leq 1$$

I_E can be treated as a function of I_A and E_b / N_0 .

To compute I_E , we must first compute the distributions of p_E (using histogram). In [19], it is approximated by time averages

$$I(X; E) \approx 1 - \frac{1}{N} \sum_{n=1}^N \log(1 + e^{-x_n \cdot E(x_n)}) \quad (4.13)$$

From the observation of simulations, it is enough to use time average (4.13)

when N is larger than 10,000 bits.

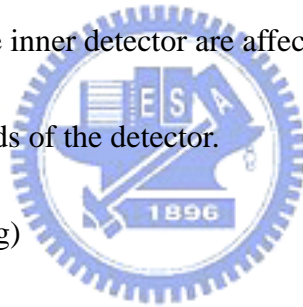
4.2 Transfer curve simulations

In this section, we show some transfer curves of both the detector and the decoder. After combining the two transfer curves into one single chart which is just called EXIT chart, we can observe the convergence behavior of the iterative decoding.

4.2.1 Transfer characteristics of the detectors

The transfer curves of the inner detector are affected by some factors:

1. The detecting methods of the detector.
2. Bit mapping (labeling)
3. E_b / N_0 (SNR)
4. Code rate R
5. Transmit and receive antenna number



Transfer characteristics for different bit mapping at fixed $E_b / N_0 = 3dB$ are depicted in Fig.4-2. The influences of different E_b / N_0 on the transfer characteristics are shown in Fig.4-3 to Fig.4-5. All curves are 16QAM mapping.

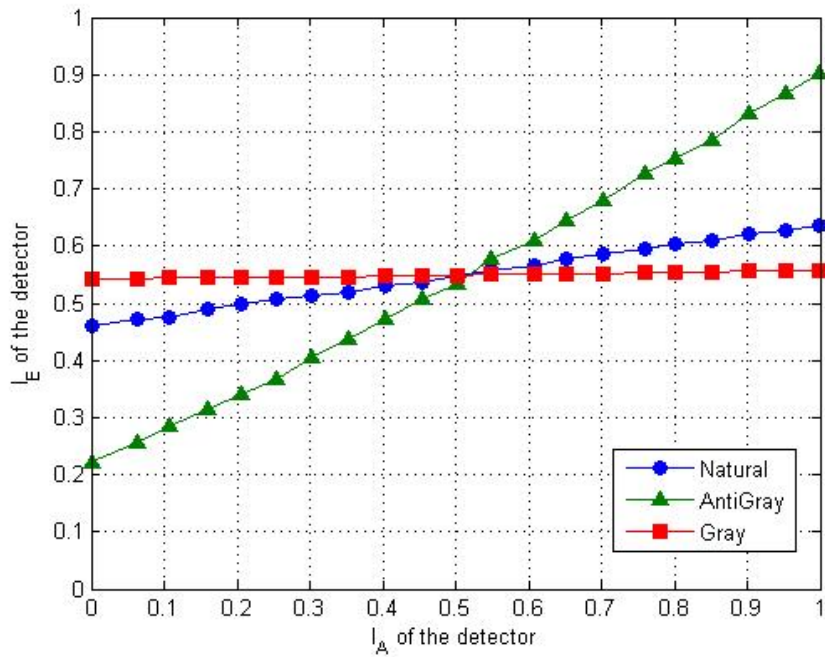


Fig. 4-2: Extrinsic information transfer characteristics of the inner detector for Natural, AntiGray and

Gray mapping at $E_b/N_0 = 3dB$ with 16QAM and single antenna.

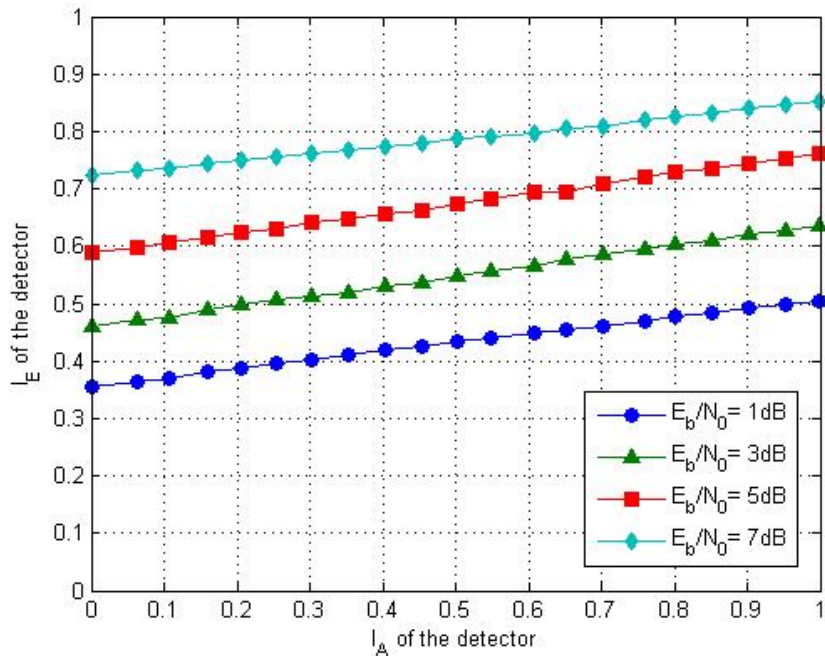


Fig. 4-3: Extrinsic information transfer characteristics of the inner detector for 16QAM, Natural

mapping at $E_b/N_0 = 1dB, 3dB, 5dB$ and $7dB$.

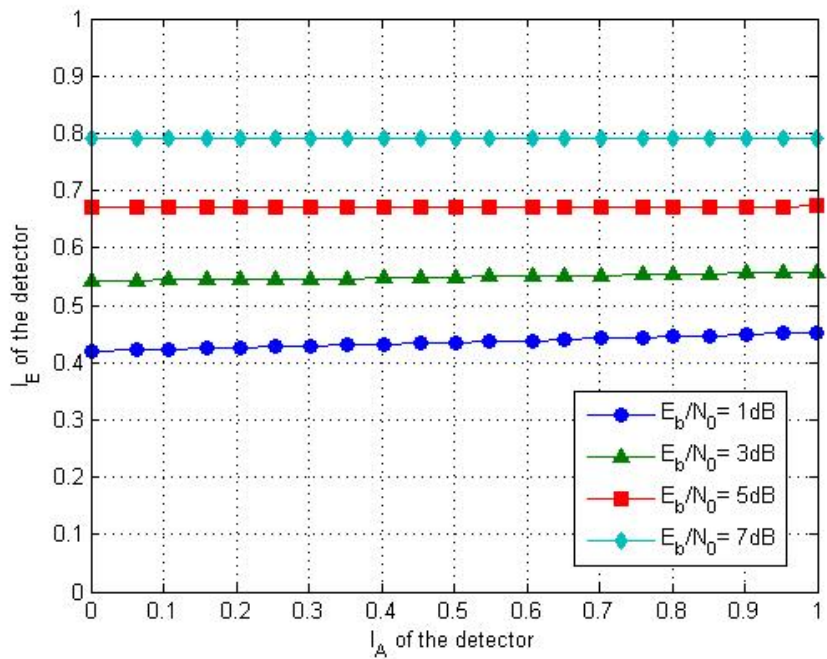


Fig. 4-4: Extrinsic information transfer characteristics of the inner detector for 16QAM, Gray mapping

at $E_b / N_0 = 1\text{dB}, 3\text{dB}, 5\text{dB}$ and 7dB

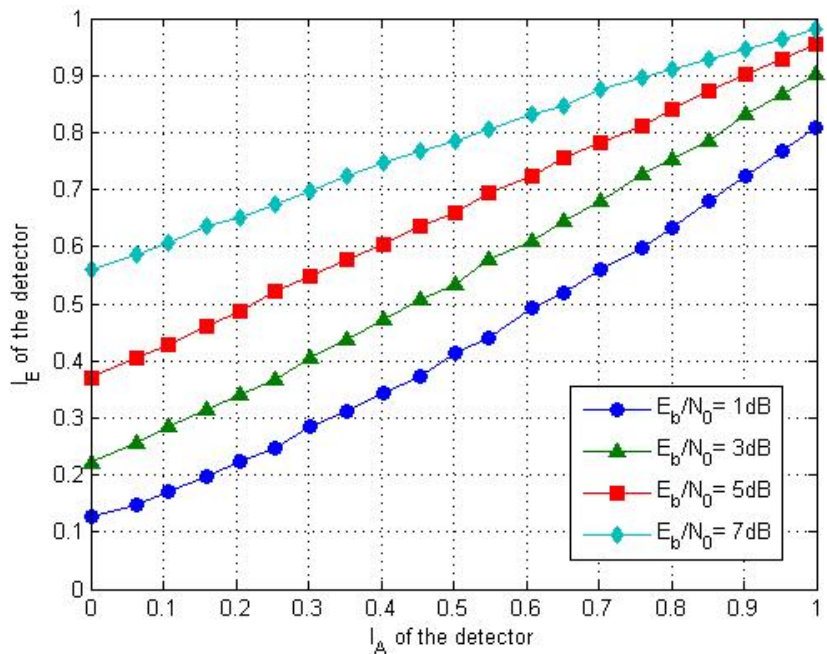


Fig. 4-5: Extrinsic information transfer characteristics of the inner detector for 16QAM, Anti-Gray mapping

mapping at $E_b / N_0 = 1\text{dB}, 3\text{dB}, 5\text{dB}$ and 7dB

4.2.2 Transfer characteristics of the decoders

In the serial concatenated system, the outer decoder only receives the log-likelihood ratio from the inner detector. Hence the transfer characteristics of the decoder is just affected by the input a priori information and the code rate. Transfer characteristics for different code polynomial with code rate 1/2 are depicted in Fig.4-6.

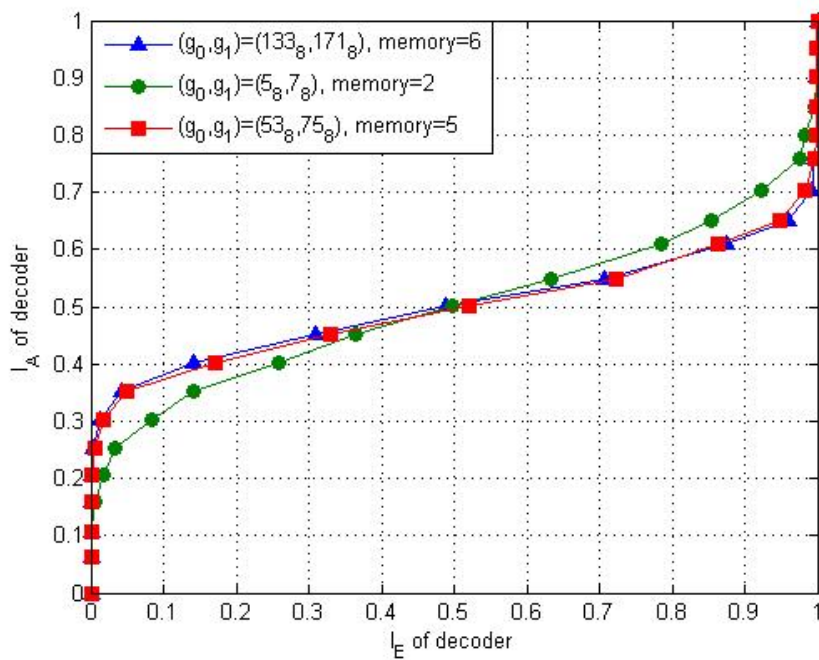


Fig. 4-6: Extrinsic information transfer characteristics of the outer decoder for different generator polynomial with code rate 1/2.

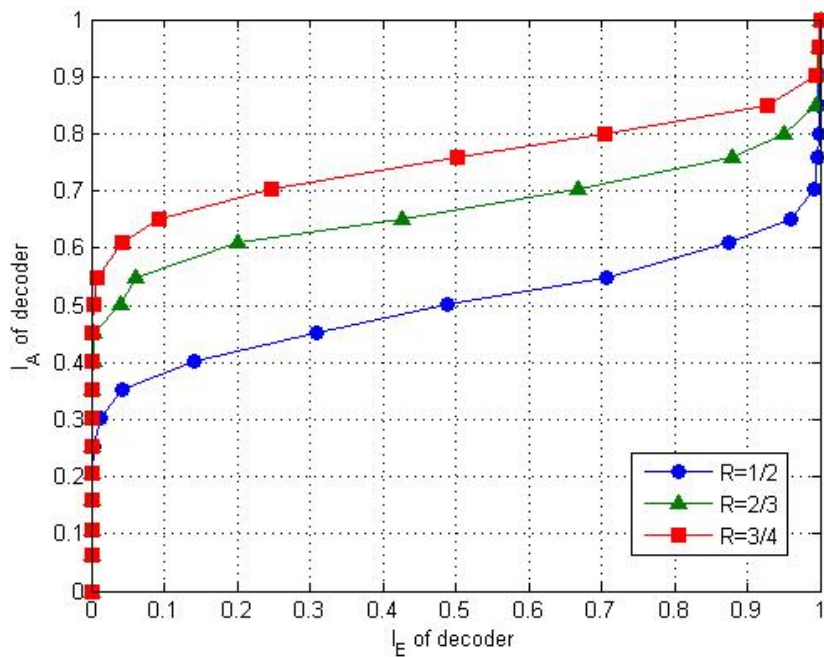


Fig. 4-7: Extrinsic information transfer characteristics of the outer decoder for the

$(133_8, 171_8)$ convolutional code with different punctured code rate.

If we puncture the convolutional code with $R=1/2$ to $R=2/3$ or $R=3/4$, transfer characteristics of the decoder will be changed. The details of puncturing convolutional codes will be discussed in chapter 6. In Fig.4-7 we just show the effects of different code rate on the transfer characteristics of the decoders.

4.2.3 EXIT chart

Combining the transfer characteristics of the detector and the decoder into one chart forms the Extrinsic Information Transfer (EXIT) chart. In the EXIT, the exchanges of the extrinsic information between the detector and the decoder are

visible. An example is depicted in Fig.4-8. The trajectory is the exchange of extrinsic information between the detector and the decoder. In Fig.4-8 we can see that the EXIT chart matches very well with the real decoding trajectory. Hence we can predict the convergence behavior with EXIT charts.

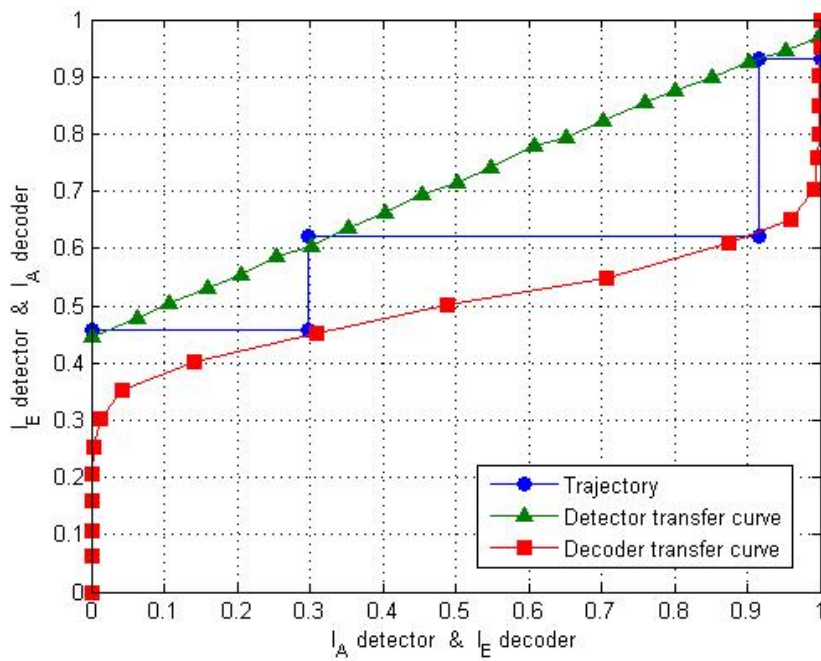


Fig. 4-8: EXIT chart of a serial concatenated system with APP detector and a $(133_8, 171_8)$ convolutional code, 16QAM and Anti-Gray mapping.